ELSEVIER

Journal of Photochemistry and Photobiology A: Chemistry 115 (1998) 81–87

Journal of Photochemistry and Photobiology A:Chemistry

Four-wave mixing studies of UV curable resins for microstereolithography

M. Farsari *, S. Huang, R.C.D. Young, M.I. Heywood, P.J.B. Morrell, C.R. Chatwin

Laser and Photonics Systems Group, School of Engineering, University of Sussex, Falmer, Brighton, BN1 9QT, UK

Received 16 January 1998; accepted 10 February 1998

Abstract

The optical characteristics of three commercial UV curable resins are investigated using non-degenerate four-wave mixing. The materials assessed are an acrylate and two epoxy resins. The holographic gratings were written at a wavelength of $\lambda = 351.1$ nm for an irradiance range 0.5–3.0 W/cm^2 and read at $\lambda = 632.8$ nm in order to compare the reactivity, curing speed, shrinkage and resolution of the resins. These experiments were carried out to prove the suitability of the photopolymerisation systems for microstereolithography.

Keywords: Microstereolithography; Four-wave mixing; Photopolymers; UV curing; Rapid prototyping; Rapid tooling

1. Introduction

In order for a resin to be suitable for stereolithographic applications, several requirements must be fulfilled. The resin must: be photosensitive at the operating wavelength; have low viscosity and produce a smooth surface; have a high curing speed (especially when the component may be constructed from several hundred layers); result in good toughness of the finished part; and have low shrinkage during the liquid to solid polymerisation process [1,2]. As the demand for ever smaller stereolithographic components increases, the dimensional accuracy achievable with the building material is increasingly important; single parts must be built with micron scale dimensions [3].

The first materials designed specifically for stereolithographic applications were acrylate resins, where these are usually mixtures of monomer and oligomer acrylates with a radical photoinitiator. This composition has several useful properties, such as high photosensitivity; oxygen inhibition, which assists smooth spreading of the material [2]; low critical energy; controllable mechanical properties; and relative insensitivity to temperature and humidity changes. The extent of their use in applications has been limited by their poor dimensional stability and by their high volume shrinkage, where the latter characteristic results in curl occurring during and after the component building process [2].

Recently a new generation of materials for stereolithography have been developed. These are based on special epoxy resins, which polymerize with the help of a cationic photoinitiator. Such materials have a lower photosensitivity than acrylate resins, a high critical energy, no oxygen inhibition and high sensitivity to temperature and humidity. However, in contrast to acrylate resins, they have exceptionally low volume shrinkage and good dimensional stability [2].

Commercially available stereolithography systems use a focused scanning laser beam to partially solidify components, layer by layer, into a honeycomb structure. Components are then fully cured in a post curing process. In these systems the maximum component accuracy is 0.1 mm, which is a limitation imposed by using a focused laser beam. We are constructing a microstereolithography machine that uses a two-dimensional dynamic electro-optic mask to modulate an Argon-ion UV laser beam. Using this approach component accuracy of 1 μm will be possible.

This study was conducted to establish resin performance and resolution characteristics for microstereolithography. We investigated one acrylate (Zeneca Stereocol™ H-N 9000) and two epoxy (Ciba-Geigy Cibatool™ SL 5170 and DuPont Somos™ 6100) resins. These commercially available resins are protected by patents and their composition is confidential. To compare their reactivity, rate of the polymerization reaction, oxygen inhibition and the extent of volume shrinkage during polymerization [4] we performed four-wave mixing holographic measurements using an Argon ion laser operat-

* Corresponding author.

1010-6030/98/$19.00
PII S1010-6030(98)00242-1

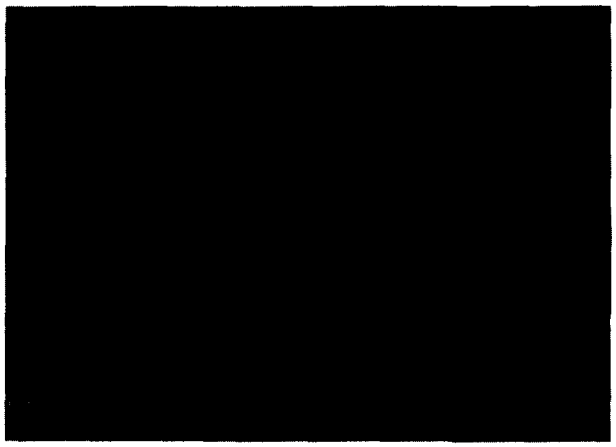

Fig. 1. 'Microbubbles' trapped in a Ciba-Geigy Cibatool™ SL 5170 non-degenerate four-wave mixing sample.

ing on the $\lambda_0 = 351.1$ nm line. It should be pointed out that only the DuPont Somos™ 6100 resin is specifically designed for this wavelength; the Zeneca Stereocol™ H-N 9000 and the Ciba-Geigy Cibatool™ SL 5170 resins have been optimized for operation at 325 nm, using a He–Cd laser. Since our project goes beyond the operational envelope of conventional stereolithography it was considered useful to know the processability of a range of materials at an Argon-ion wavelength.

2. Sample preparation

The samples were prepared and all measurements were taken in a controlled environment using a temperature of $T = 19$°C and humidity of 50%–60%. The preparation of the samples involved placing a drop of resin between two glass plates separated by 0.1 mm thick Mylar spacers. All the measurements were taken within four hours of the formation of the samples.

Some of the samples demonstrated a lot of scattering when illuminated by laser light. There was no imperfection visible to the naked eye but when looked at under a microscope, very small bubbles were evident (Fig. 1). The effect was smaller in the Ciba-Geigy Cibatool™ SL 5170 samples, which was probably due to the lower viscosity of this resin (see Table 1). For the measurements, only the samples that transmitted a uniform beam were used, where these were then examined after the experiment for 'bubble trapping'.

3. Experimental set-up

The principles of non-degenerate four-wave mixing are described in Refs. [5,6]. Our experimental set-up is shown in Fig. 2. An Ar-ion laser with beam diameter $R = 1.57$ mm (specified at the $1/e^2$ points) and operating at $\lambda_0 = 351.1$ nm was used to polymerize the resin. The laser beam was split into two equal power beams I_r and I_s using a quartz cube beam splitter. The two beams overlap in the sample, generating an interference pattern:

$$I(x) = I_0(1 + m\cos(kx)) \quad (1)$$

$I_0 = I_s + I_r$ is the maximum irradiance, $m = 2(I_r I_s)^{1/2}(I_r + I_s)^{-1} = 1$ is the modulation index and k is the spatial

Table 1
The viscosity and the refractive index of the investigated materials

Material	Viscosity [a] (cps, 30°C)	Refractive index
Ciba-Geigy Cibatool™ SL 5170	165–195	1.49 ± 0.05
Zeneca Stereocol™ H-N 9000	1070	1.49 ± 0.05
DuPont Somos™ 6100	250	1.52 ± 0.05

[a] Information provided by the manufacturers' data sheets.

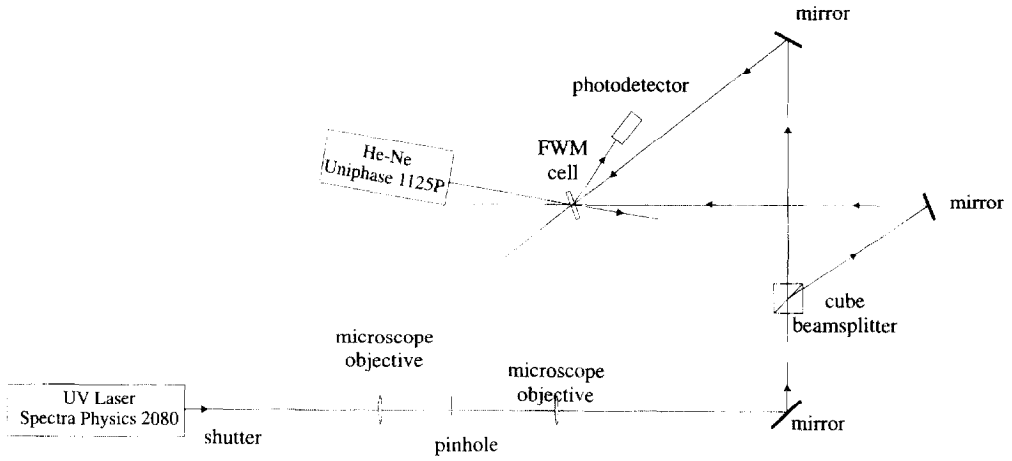

Fig. 2. Experimental set-up for non-degenerate four-wave mixing.

frequency of the grating. The spatial wavelength Λ_G is given by the relation

$$\Lambda_G = \frac{\lambda_0}{2n \sin(\theta_0)} \quad (2)$$

where $2\theta_0$ is the angle between the two beams and n is the refractive index of the material. The beams are controlled by an electronic shutter with a closure response time of 6 ms.

The grating was read using a 5 mW He–Ne laser operating at $\lambda = 632.8$ nm, with the plane of polarization perpendicular to the plane of incidence. The resins are not reactive at this wavelength and as a result this beam does not contribute to the creation of a grating. The diffracted beam is detected using a silicon photodiode, connected to a LeCroy 9361 digital storage oscilloscope.

If the response of the material is linear with the beam intensity, the light pattern produces a refractive index grating

$$n(x) = n_0 + \frac{1}{2}\Delta n(1+\cos(kx)) \quad (3)$$

where Δn is the amplitude change in the refractive index.

The grating diffraction efficiency η is defined as the ratio of the intensity of the diffracted beam over the intensity of the incident beam. If Δn is small and there is no change in the absorption constant α of the material during polymerization, then it can bee approximated by the Kogelnik relation [7]

$$\eta = \exp(-ad/\cos\theta)\sin^2\left(\frac{\pi \cdot \Delta n \cdot d}{\lambda \cos\theta}\right) \quad (4)$$

where $d = 100$ μm is the thickness of the sample and θ is the angle of incidence of the reading beam. λ and θ satisfy the Bragg condition.

$$2\Lambda \sin\theta = \lambda \quad (5)$$

The change in the refractive index is due to the change of the density of the material (shrinkage). There has been no proof of a direct relation between volume shrinkage and curl occurring in the cured material. This is mainly because it is almost impossible to find material formulations that differ only in curl shrinkage, while leaving other parameters unchanged [1]. It is, however, safe to assume that a high diffraction efficiency would indicate high curl during building.

The induced refractive index change in UV curable photopolymers is nonlinear with respect to the illuminating irradiance. The refractive index grating that results from the sinusoidal fringe pattern generated by the interference of the two writing beams can be more closely represented as a square wave grating which leads to higher order terms in the wave diffracted from the grating [6]. However, it has been shown that for small grating amplitudes [8], the Kogelnik formula is a good approximation for the relation between the first order diffraction efficiency η_1 and the amplitude of the first harmonic grating Δn_1.

4. Results

In order to calculate the grating spacing Λ and Bragg angle θ from Eqs. (2) and (5), respectively, the refractive indices of the resins must be known. They were measured using an Abbé refractometer and are presented in Table 1.

The nonlinear behaviour of the materials investigated was confirmed by the presence of a second order diffracted beam (Fig. 3). It became evident from the experiment that the low critical energy of the acrylate Zeneca Stereocol™ H-N 9000 was a disadvantage. Whereas in the case of the epoxy resins there was a well-defined interface on the samples, where the liquid had been exposed to the UV beam and solidified; for the acrylate resin, a much larger area was affected, this being due to scattered radiation. This could have important implications when this material is used in microstereolithography, since the effect of scattering would make it difficult to achieve the dimensional accuracy required to build microcomponents.

Fig. 4 shows the time history diagrams of the three resins where the diffraction efficiency is plotted versus irradiation time. It is presented as a normalized logarithmic diagram of the evolution of the diffraction efficiency over 45 s, to compare the different responses of the three materials. The power of each of the writing beams was 10 mW and the angle between the two writing beams is $2\theta_0 = 24°$.

It is evident that the DuPont Somos™ 6100 has a completely different response to that of the other two resins. That is to say, the Ciba-Geigy Cibatool™ SL 5170 and the Zeneca Stereocol™ H-N 9000 resins rise to a maximum diffraction efficiency which then decreases. This type of response is similar to previous reports which have used four-wave mixing to assess UV-curable resins [4,8]. The DuPont Somos™ 6100, however, demonstrates an initial peak in the diffraction efficiency, a decrease followed by a slow increase to the final value.

Fig. 3. Nondegenerate four-wave mixing. From left to right, the arrows point to the reading beam, the first-order diffracted beam and the second-order diffracted beam.

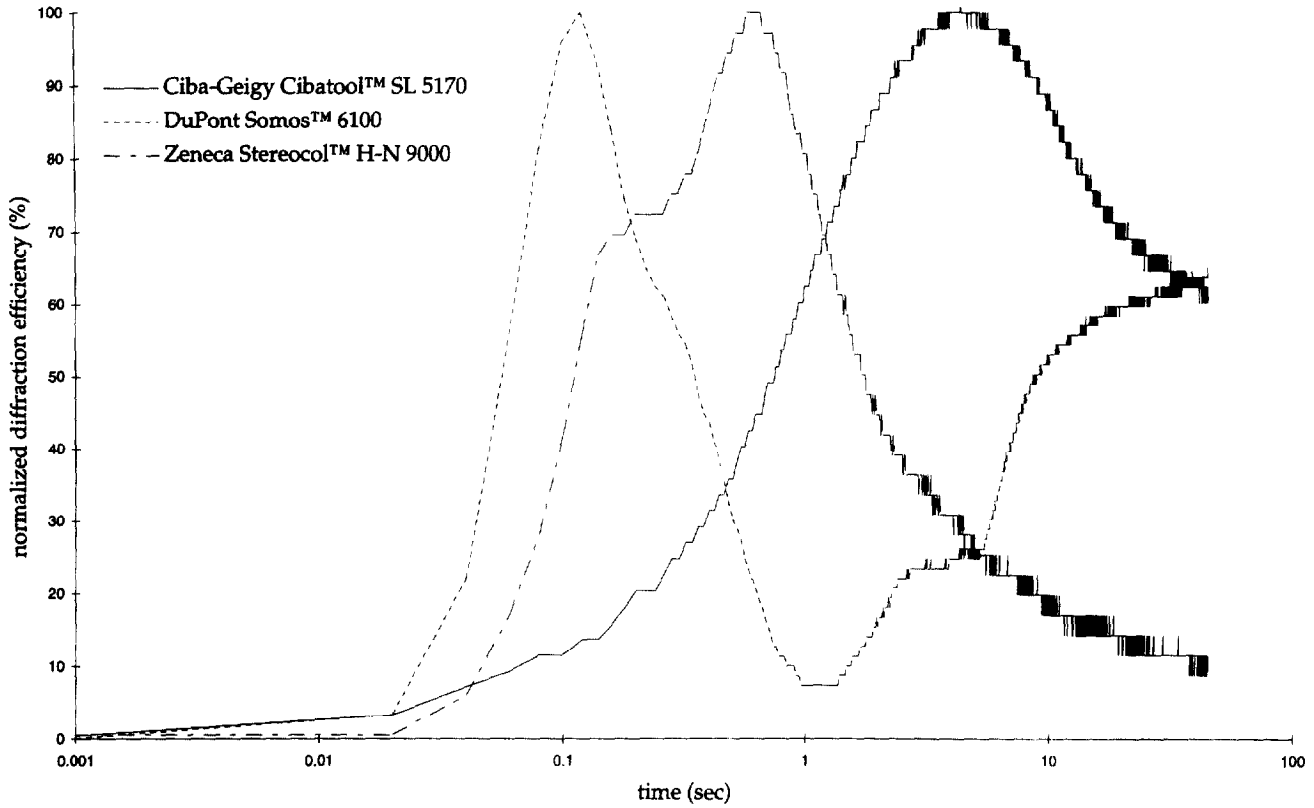

Fig. 4. Time evolution of the diffraction efficiency.

In order to further investigate this behaviour, exposure times shorter than the initial rise time of the diffraction efficiency were used. The result of this was that the shape of the slope did not change; however the final diffraction efficiency was lower. If the writing beams were blocked after the initial peak, then the diffraction efficiency would evolve as in Fig. 4. This leads us to believe that the first peak is due to the creation of the cations in the material, while the second rise in the diffraction efficiency is due to the polymerization which, in the case of DuPont Somos® 6100, is much slower than the initial cation creation. As the polymerization of the material occurs regardless of the continuation of UV irradiation, curing time should be regarded as the time to the initial peak in the diffraction efficiency.

Plotting diffraction efficiency versus time therefore provides information about the delay time until the onset of diffraction, the final value of the diffraction efficiency and the rate of increase of diffraction. This information is discussed in Sections 4.1, 4.2 and 4.3.

4.1. Delay

The delay time t_0 characterizes a system in terms of oxygen inhibition and photosensitivity. During this time the dissolved oxygen in the system is consumed by the radicals generated by the irradiation of the sample. Once the oxygen is consumed, polymerization starts and the holographic grating forms. The rise time to 10% of the maximum diffraction efficiency versus the beam power, for the three resins investigated, is plotted in Fig. 5.

It was not a surprise that the DuPont Somos® 6100 resin gave the shortest delay time. The epoxy resin is not only oxygen absorption inhibited but the DuPont Somos® 6100 is also designed to provide maximum sensitivity at 351.1 nm. The experiments also demonstrated that this resin was not significantly affected by the beam power.

The acrylate Zeneca Stereocol® H-N 9000 resin showed a delay time higher than that of the DuPont Somos® 6100 resin, but was still fairly insensitive to changes in beam power. In this case the delay can be attributed to both oxygen absorption and wavelength insensitivity.

The Ciba-Geigy Cibatool® SL 5170 resin, also an epoxy resin, showed the largest delay time. As oxygen inhibition cannot account for this, we can only assume that the sensitivity of this resin at this wavelength is low. The delay decreases very rapidly with increasing laser power, becoming lower than the Zeneca Stereocol® H-N 9000 for beam irradiance greater than 1.5 W/cm^2.

4.2. Diffraction efficiency

The diffraction efficiency of the three resins was measured for different beam powers and grating spacing, thirty seconds after the opening of the beam shutter, when the diffraction had reached a constant value. For beam irradiances in the 0.5–3.0 W/cm^2 range investigated, it was observed that the

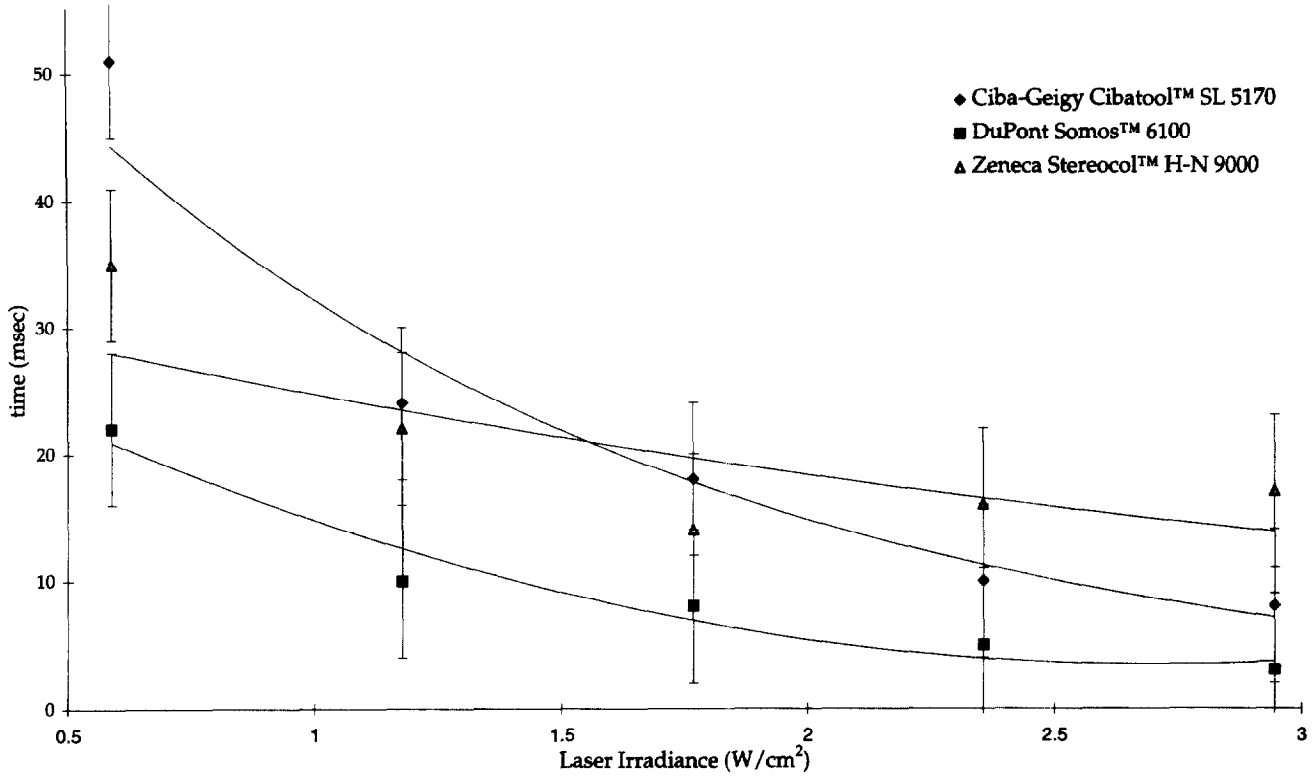

Fig. 5. Dependence of the diffraction delay on the writing beam irradiance.

magnitude of the irradiance did not affect the diffraction efficiency. The variation of the diffraction efficiency with grating spacing is shown in Fig. 6.

As previously indicated, a high diffraction efficiency is synonymous with a high curl distortion, and it is expected that acrylate resins have a higher curl distortion than epoxy

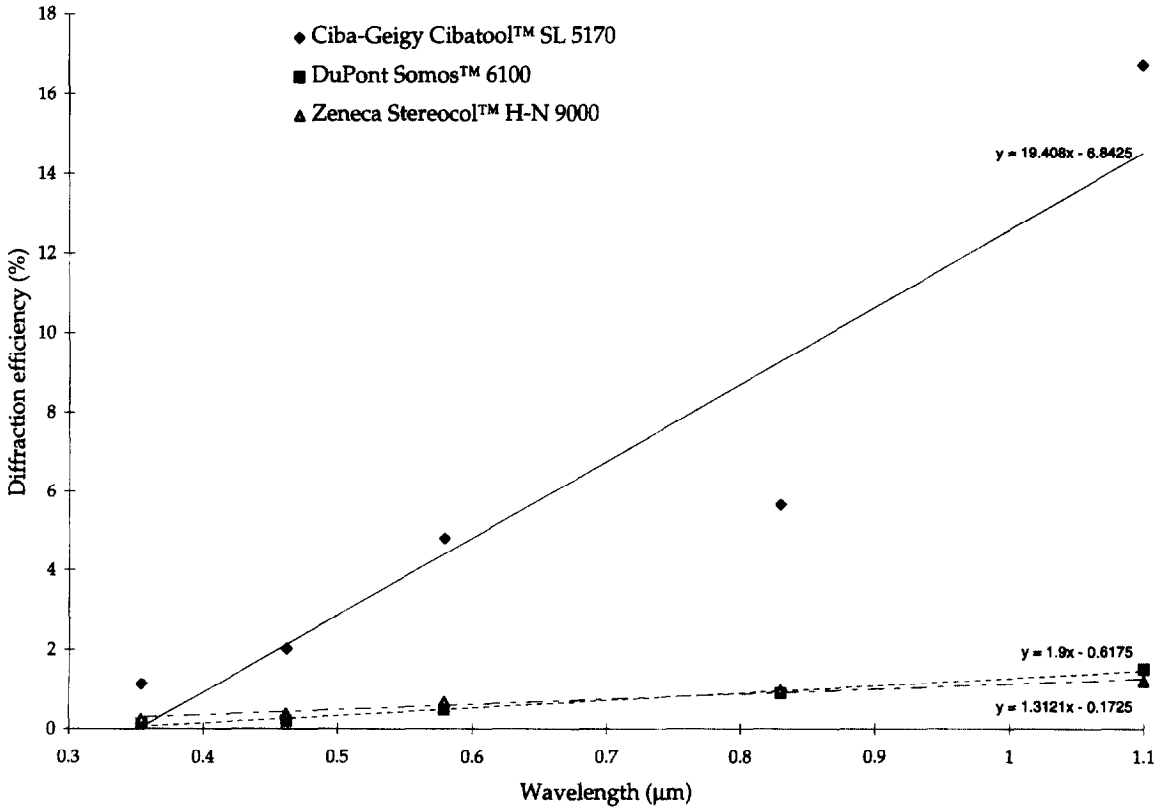

Fig. 6. Dependence of the diffraction efficiency on the spatial wavelength.

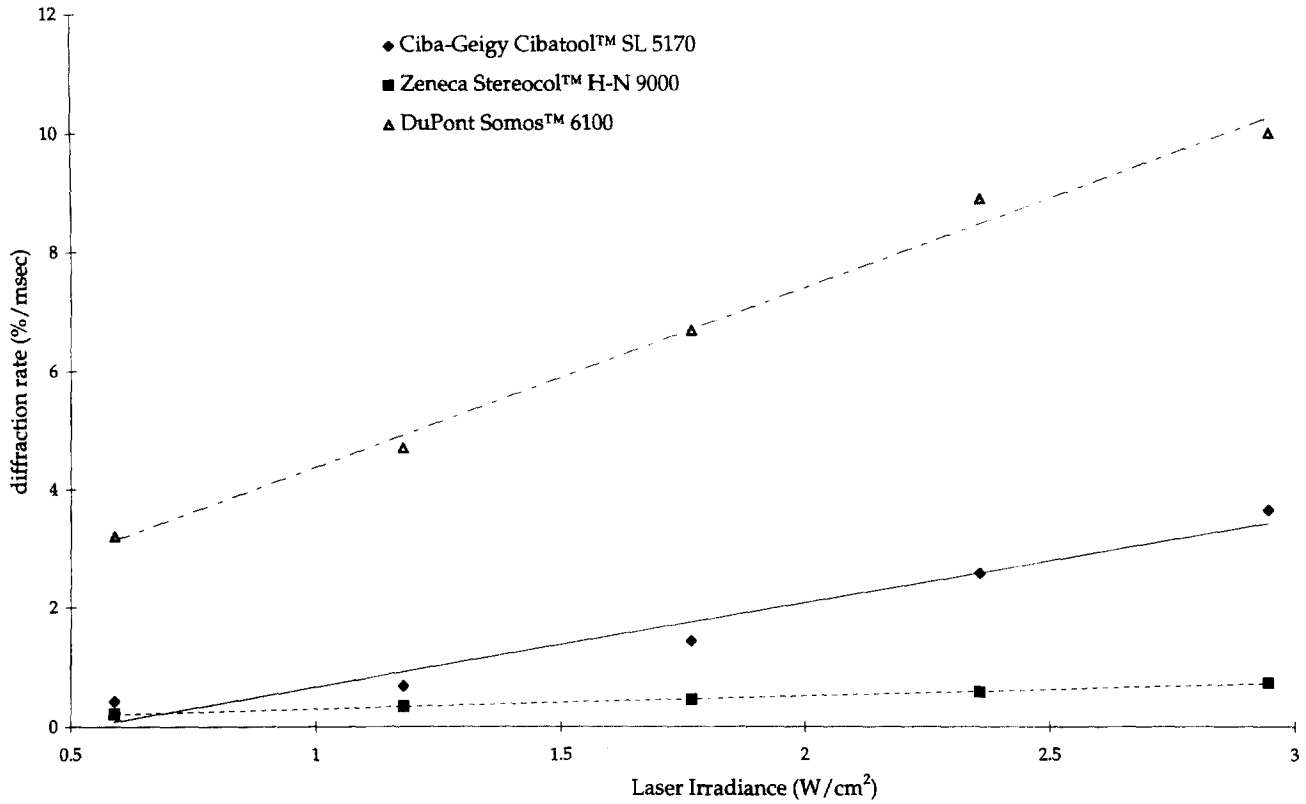

Fig. 7. Dependence of the diffraction rate on writing beam irradiance.

resins. DuPont Somos® 6100 and Zeneca Stereocol® H-N 9000 gave similar results, but this can be explained by the fact that the latter resin is much more viscous than the former (it is a well-known fact that the more dilute the solution, the greater the possibility of the final component fracturing due to shrinking effects). Low viscosity can perhaps explain why the Ciba-Geigy Cibatool® SL 5170, even though it is an epoxy resin, has a diffraction efficiency an order of magnitude higher than the other two materials investigated.

From Fig. 6, it is observed that the diffraction efficiency decreases when the spatial wavelength decreases. This is due to the reduction of the modulation index, caused by the limited resolution of the material. It is noted that the largest drop is in the case of the Ciba-Geigy Cibatool® SL 5170 resin, followed by DuPont Somos® 6100 and finally Zeneca Stereocol® H-N 9000. Overall, however, the resolution of all the materials investigated were exceptionally high. Specifically, it was possible to write (but not measure) gratings with a fringe period of 0.28 μm, which corresponds to a feature size of 0.14 μm. Since most stereolithographic machines require an accuracy in the order of millimeters, the resolution of the investigated resins is more than adequate for their intended purpose.

In our microstereolithography project we require 1 μm resolution, hence, as far as resolution is concerned, all three resins were found to be suitable.

4.3. Rate

The rate at which diffraction efficiency increases is an indication of the reactivity of the resin. This gives information about the reaction rate of the double bonds of the monomers and oligomers that constitute the resin. Unfortunately, since the composition of the materials is not known, it is impossible for us to calculate how many reactions correspond to each photon of UV radiation. Hence, the following comments are limited to a comparison between the resins. Their diffraction rate as a function of the irradiance of the writing beams is shown in Fig. 7.

It is generally expected that acrylate resins are faster than epoxy resins [4]; however measurements indicated that the Zeneca Stereocol® H-N 9000 is the slowest of the materials investigated. DuPont Somos® 6100 was by far the fastest which is attributable to the wavelength specific tuning engineered by the manufacturers. In all cases the diffraction rate increased linearly with irradiance.

5. Discolouration

A common problem with UV curable resins is the change of the absorption of the material whilst curing. This is particularly significant within the context of rapid prototyping, as

a decrease in the absorption (bleaching) would allow light to pass into masked areas of previously exposed layers.

In order to investigate this effect, a simple experiment was conducted; the transmission of a He–Ne laser beam through a resin sample was monitored as the sample was exposed to UV radiation. The samples used were similar to the ones for the nondegenerate four-wave mixing. In all cases the transmission of the He–Ne beam decreased, which indicates an increase in the absorption of the resin as it was cured. This decrease was no more than 1–2%, and is therefore not expected to significantly influence the fabrication of rapid prototyping components.

6. Conclusions

All the materials investigated demonstrated their ability to give high build resolution and are suitable for microstereolithography applications. Tuning the resin properties so as to be optimized for the specific curing wavelength is clearly important to maximize cure speed and minimise shrinkage. For this reason the DuPont Somos™ 6100 performed best at the wavelength employed. However the Ciba-Geigy Cibatool™ SL 5170 gives better processability via reduced 'bubble trapping'. This is particularly important for microstereolithography as feature sizes are likely to be comparable with the size of the entrapped bubbles.

Acknowledgements

We gratefully acknowledge the Engineering and Physical Sciences Research Council for their support of this research.

References

[1] P.F. Jacobs, Rapid Prototyping and Manufacturing, CASA-SME, 1992.
[2] A. Schulthess, B. Steinmann, M. Hofmann, Proceedings of the 28th International Symposium on Automotive Technology and Automation—Rapid Prototyping in the Automotive Industries, 1995, p. 41.
[3] A. Bertsch, J.Y. Jézéquel, J.C. André, J. Photochem. Photobiol. A: Chem. 107 (1997) 275.
[4] M. Hunziker, P. Bernhard, Proceedings of the 1st National Conference on Rapid Prototyping, Dayton, OH, 1990, p. 79.
[5] C. Braüchle, D.M. Burland, Angew. Chem., Int. Ed. Engl. 22 (1983) 582.
[6] C. Carré, D.J. Lougnot, J.P. Fouassier, Macromolecules 22 (1989) 791.
[7] H. Kogelnik, Bell. Syst. Tech. J. 48 (1969) 2909.
[8] J. Marotz, Appl. Phys. B 37 (1985) 181.